Published in final edited form as:
J Neurophysiol. 2007 May ; 97(5): 3365–3375.

Metabotropic Glutamate Receptors in the Lateral Superior Olive Activate TRP-Like Channels: Age- and Experience-Dependent Regulation

F. Aura Ene, **Abigail Kalmbach**, and **Karl Kandler**
Department of Neurobiology and Center for the Neural Basis of Cognition, University of Pittsburgh School of Medicine, Pittsburgh, Pennsylvania

Abstract

The lateral superior olive (LSO) is the primary auditory nucleus for processing of interaural sound level differences, which is one of the major cues for sound localization. During development, survival and maturation of LSO neurons critically depend on synaptic activity and intracellular calcium signaling. Before hearing onset, glutamatergic synaptic inputs from the cochlear nucleus (CN) to the LSO activate group I metabotropic glutamate receptors (mGluRs), which leads to calcium release from intracellular stores and large calcium influx from the extracellular milieu. Here, we investigated the nature of the mGluR-activated membrane channel that mediates the influx of ex-tracellular calcium. Using Fura-2 calcium imaging in brain stem slices of neonatal and juvenile mice, we found that this calcium channel is blocked by Ni^{2+}, La^{3+}, and 2-aminoethoxydiphenylborane (2-APB), known antagonists of transient receptor potential (TRP) channels. During postnatal development, the contribution of extracellular calcium influx to mGluR-mediated Ca^{2+} responses gradually decreased and was almost abolished by the end of the third postnatal week. Over this period, the contribution of Ca^{2+} release from internal stores remained unchanged. The developmental decrease of TRP-like channel-mediated calcium influx was significantly less in congenitally deaf waltzer mice, suggesting that early auditory experience is necessary for the normal age-dependent downregulation of functional TRP channels.

INTRODUCTION

The lateral superior olive (LSO) is a binaural auditory brain stem nucleus involved in the processing of interaural sound level differences. LSO neurons receive excitatory, glutamatergic inputs from the ipsilateral cochlea by the anteroventral cochlear nucleus (AVCN) and inhibitory, glycinergic inputs from the contralateral cochlea by the medial nucleus of the trapezoid body (MNTB) (Boudreau and Tsuchitani 1968; Oertel 1999; Tollin 2003). Both inputs are tonotopically organized and aligned, which enables LSO neurons to process binaural inputs in a frequency-specific manner (Sanes and Rubel 1988; Tollin 2003).

During development, the LSO circuit undergoes a number of morphological and functional changes that include growth and refinement of dendritic arbors (Rietzel and Friauf 1998; Sanes et al. 1992), functional and structural refinement of the MNTB–LSO pathway (Kandler and Gillespie 2005; Kim and Kandler 2003; Sanes and Siverls 1991; Sanes and Takacs 1993), and a switch in neurotransmitter phenotype (Gillespie et al. 2005; Kotak et al. 1998; Nabekura et al. 2004). Many of these processes occur before hearing onset but nevertheless depend on

Address for reprint requests and other correspondence: K. Kandler, Department of Neurobiology, University of Pittsburgh School of Medicine, Biomedical Science Tower W1457, 3500 Terrace Street, Pittsburgh, PA 15261 (E-mail: kkarl@pitt.edu).

neuronal activity and intracellular Ca^{2+} signaling (Friauf and Lohmann 1999; Kotak and Sanes 2000; Lohmann et al. 1998; Sanes and Siverls 1991; Sanes and Takacs 1993).

Before hearing onset, spontaneous neuronal activity is present in the form of high-frequency bursts at various levels in the auditory pathway (Glowatzki and Fuchs 2000; Gummer and Mark 1994; Jones et al. 2001; Kotak and Sanes 1995; Kros et al. 1998; Lippe 1994; Romand and Ehret 1990). In the prehearing mouse, activation of glutamatergic cochlear nucleus (CN) inputs onto LSO neurons elicits postsynaptic Ca^{2+} responses that are mediated by ionotropic and metabotropic glutamate receptors (mGluRs). The recruitment of specific types of glutamate receptors depends on the spatial and temporal patterns of synaptic activation (Ene et al. 2003). Burstlike synaptic activity activates group I and group II mGluRs, which in turn generate postsynaptic Ca^{2+} responses with a typical biphasic profile. The initial phase of mGluR-elicited Ca^{2+} responses in immature LSO neurons is mediated by Ca^{2+} release from intracellular stores, whereas the later and prolonged phase is mediated by an influx of extracellular Ca^{2+} through membrane Ca^{2+} channels.

The identity of mGluR-activated membrane Ca^{2+} channels in LSO neurons is unclear, although their dependency on intracellular Ca^{2+} release suggests that they belong to the family of transient receptor potential channels (TRPCs) (Clapham 2003; Montell 2005), which can be activated by mGluRs (Bengtson et al. 2004; Gee et al. 2003; Kim et al. 2003; Tozzi et al. 2003). In this study, we investigated the developmental changes of mGluR-mediated Ca^{2+} responses in mouse LSO neurons and characterized the pharmacological properties of the mGluR-activated Ca^{2+} channel. We found that the pharmacological profile of mGluR-activated Ca^{2+} channels is consistent with the characteristics of a TRPC. During the first three postnatal weeks, group I mGluR-evoked Ca^{2+} responses decreased, with the most pronounced changes occurring around the onset of hearing when mGluRs ceased to trigger extracellular Ca^{2+} influx. These developmental changes were delayed in congenitally deaf waltzer mice, suggesting that developmental downregulation of TRP-like Ca^{2+} responses is influenced by normal auditory experience.

METHODS

Animals

Experiments were performed in C57BL/6J and homozygote waltzer Cdh23 mice (C57BL/6J-*Cdh23*$^{v-2J}$) of both genders (Jackson Laboratory, Bar Harbor, ME; Charles River, Wilmington, MA), ages between postnatal day 0 (P0: the day of birth) and P20. Waltzer homozygotes were identified by their rollover behavior deficits (Wada et al. 2001). Heterozygote mice were obtained by breeding homozygote/wild-type pairs. All experimental procedures were in accordance with National Institutes of Health guidelines and were approved by the Institutional Animal Care and Use Committee at the University of Pittsburgh.

Slice preparation

Animals between P0 and P7 were anesthetized by hypothermia and animals older than P7 were anesthetized using isoflurane. Animals were quickly decapitated and the brains were removed and placed into cold (4–8°C) artificial cerebrospinal fluid with kynurenic acid [ACSF with KA, composition (in mM): NaCl 124, $NaHCO_3$ 26, glucose 10, KCl 5, KH_2PO_4 1.25, $MgSO_4$ 1.3, $CaCl_2$ 2, and kynurenic acid 1; pH 7.4 when aerated with 95% O_2-5% CO_2]. Transversal, 200- to 300- μm-thick slices of the brain stem were cut with a vibrotome (DTK-1500E, Ted Pella, Redding, CA) and slices containing the LSO were used for Fura-2 labeling.

Fura-2 labeling

Slices from P0 to P7 animals were labeled with an acetoxymethyl ester of Fura-2 (Fura-2 AM), using bulk-labeling, as described previously (Ene et al. 2003). In slices from animals older than P7 LSO neurons labeled poorly or not at all, using the bulk-labeling method, most likely resulted from poor penetration of Fura-2 AM through the extracellular matrix. Therefore slices from P9 to P20 were labeled using a novel spin-labeling procedure. Slices were placed on filter paper (12-μm pores; Corning Life Sciences, Acton, MA) in an interface-type chamber and after 15–30 min were transferred into a microcentrifuge tube equipped with a 10-kDa cutoff molecular filter (Amicon; Millipore, Bedford, MA). Slices were covered with 100 μM Fura-2 AM in ACSF and aerated with 95% O_2-5% CO_2. The micro-centrifuge tube was centrifuged for 15–20 min at about 430 *g* (IEC Clinical Centrifuge; International Equipment, Needham Heights, MA), forcing the Fura-2 AM solution to pass through the slice. Slices were then removed from the microcentrifuge tube, immediately washed with freshly aerated ACSF, and kept in an interface chamber in the dark at room temperature (22–25°C) until used for Ca^{2+} imaging.

Calcium imaging

Ca^{2+} imaging was performed using an inverted epifluorescence microscope (Nikon Eclipse TE200) equipped with ×10 and ×20 air objectives [numerical aperture (NA): 0.5 and 0.75, respectively] as previously described (Ene et al. 2003). Slices were continuously superfused with oxygenated ACSF at 30–32°C (perfusion rate 2–3 ml/min) containing 100 μM Trolox to minimize photodamage (Scheenen et al. 1996). Fluorescence images were acquired every 5–10 s with a 12-bit, cooled, interline-transfer CCD camera (IMAGO; T.I.L.L. Photonics, Martinsried, Germany) using alternating excitation (duration 20–50 ms) at 340 and 380 nm (Polychrome II; T.I.L.L. Photonics).

In some experiments, Fura-2 fluorescence was converted to intra-cellular Ca^{2+} concentrations ($[Ca^{2+}]_i$) as previously described (Ene et al. 2003) using the equation: $[Ca^{2+}]_i = K_d\beta(R - R_{min})/(R_{max} - R)$, where R_{min} is the fluorescence ratio of Ca^{2+} free Fura-2, R_{max} is the ratio of Ca^{2+} bound Fura-2, β is the ratio of the fluorescence intensity of Ca^{2+} free Fura-2 at 380 nm to the fluorescence intensity of Ca^{2+}-bound Fura-2 at 380 nm (Grynkiewicz et al. 1985). The Ca^{2+} K_d value for Fura-2 was taken as 224. R_{min} and R_{max} were determined by incubating the slices first in Ca^{2+}-free ACSF (Ca^{2+} was replaced with an equimolar concentration of Mg^{2+}) with 2 mM EGTA and 4 β M Ca^{2+} ionophore Br-A23187 (Alomone Labs, Jerusalem, Israel). $CaCl_2$ (10 mM) was then added to determine R_{max}. The imaging system was calibrated repeatedly over the course of this study and R_{min} varied from 0.25 to 0.31, R_{max} varied from 1.22 to 1.8, and β varied from 2.3 to 3.7.

Drug application

Drugs from concentrated stock solutions were dissolved in ACSF and delivered by bath application. Group I mGluRs were stimulated using the specific agonist (*S*)-3,5-dihydroxyphenylglycine (DHPG 20–50 μM). All experiments were performed in the presence of antagonists of ionotropic GluRs, glycine receptors, and μ-aminobutyric acid type A ($GABA_A$) receptors. Ionotropic GluRs were blocked by 6-cyano-7-nitroquinoxaline-2,3-dione disodium (CNQX, 20 μM; Tocris, Ballwin, MO) and D-2-amino-5-phosphonopentanoic acid (D-APV, 100 μM, Tocris). Glycine receptors were blocked by strychnine (10 μ M; Sigma, St. Louis, MO) and $GABA_A$ receptors were blocked by bicuculline (10 μM; Tocris). Tetrodotoxin (TTX, 1 μM; Alomone Labs) was added to block glutamate release resulting from spontaneous action potentials. For TRPC antagonists we used Ni^{2+}, La^{3+} (Sigma, St. Louis, MO), and 2-APB (Calbiochem, San Diego, CA).

Data analysis

Series of 340- and 380-nm paired images were low-pass filtered (Gaussian 3 ×3 kernel) and the background was subtracted using the program Tillvision (T.I.L.L. Photonics) as described previously (Ene et al. 2003). Ca^{2+} responses were monitored and measured from the soma of neurons. Cells with high resting $[Ca^{2+}]_i$ (>250 nM, indicating unhealthy cells) (Zirpel and Rubel 1996), cells in which the Fura-2 signal was saturated ($[Ca^{2+}]_i$ >1.5 μM, because Fura-2 does not faithfully report $[Ca^{2+}]_i$ >1.5–2 μM), and cells in which $[Ca^{2+}]_i$ did not return to baseline after stimulation were excluded from analysis. Changes in $[Ca^{2+}]_i$ that exceeded 2 SDs of the baseline and changes in $\Delta R/R > 0.1$ were considered as responses. Excel (Microsoft, Redmond, WA), Origin (OriginLab, Northampton, MA), and Matlab (The MathWorks, Natick, MA) were used for data analysis.

Responses elicited by the specific group I mGluR agonist DHPG (50 μM, 90 s) were quantified and categorized using the following parameters: peak amplitude, plateau amplitude, duration, and area under the curve. Traces were aligned to the onset of the response that was considered time 0. Baseline $[Ca^{2+}]_i$ was determined as the average of five data points before response onset (in the window −50 to 0 s). Peak amplitude was measured in the time window 0 to 40 s. Plateau amplitude was determined by averaging three to five data points in the window 80 to 100 s. Response duration was measured from the onset of the response until the response returned to baseline. Based on these measurements, responses were classified into three response types (Table 1, *n*Fig. 2): peak and plateau (pp), peak small plateau (psp), and peak no plateau (pnp). In pp responses the peak response was followed by a clear plateau (peak amplitude 236 ± 50 nM; plateau amplitude 107 ± 22 nM, = 287 cells), with a duration that always exceeded the 90-s duration of drug application (182 ± 13 s, n = 287 cells). In pnp responses the plateau phase was completely missing, the peak amplitude was small (60 ± 8 nM, n = 177 cells), and the duration was always shorter than the duration of drug application (70 ± 3 s, n = 177 cells). The intermediate group of psp responses was characterized by a gradually decreasing plateau phase, which always exceeded the duration of drug application (141 ± 15 s, n = 124 cells).

Statistical analysis

Statistical significance was analyzed using paired *t*-test, ANOVA followed by Student–Newman–Keuls post hoc test, Fisher's exact test, linear (Pearson) correlation test, Mann–Whitney nonparametric statistical test, Kolmogorov–Smirnov (KS) test, and chi-square test. Values of $P < 0.05$ were considered significant. Throughout the text, values are expressed as means > SE.

RESULTS

Group I mGluR-elicited Ca^{2+} responses were analyzed in 738 LSO neurons from 51 C57Bl6 mice (ages between P0 and P19), in 60 LSO neurons from six heterozygote waltzer mice, and in 156 LSO neurons from 14 waltzer Cdh23 homozygote mice (ages between P11 and P20). All cells included in the analysis responded to KCl-evoked depolarizations (60 mM, 30 s) with peak amplitudes ranging from about 100 nM to Fura-2–saturating responses (>1.5 μM).

Spin-labeling of LSO neurons in older slices

To overcome the poor labeling with Fura-2 AM of slices from animals older than P7 we developed a new method, *spin-labeling*, which uses centrifugation to force Fura-2 AM into the slice. To evaluate whether this new method affects Ca^{2+} responses of LSO neurons, the two labeling methods were compared in slices from P0–P5 animals. At this age, both methods produced a similar number of cells loaded with Fura-2 (bulk-labeling: n = 7.39 ± 0.92 cells/100 μm^2, n = 7 slices; spin-labeling: n = 7.98 ± 0.37 cells/100 μm^2, n = 3 slices; *t*-test $P > 0.05$)

and a similar somatic fluorescence intensity at 360 nm, the isosbestic point of Fura-2, measured with identical settings (bulk-labeling: 338 ± 67 AU, $n = 7$ slices; spin-labeling: 272 ± 108 AU, $n = 3$ slices; *t*-test, $P > 0.05$; Fig.1A). Resting somatic Ca23 concentrations were not significantly different (bulk-labeling: 94.2 3 47.6 nM, n 3 96 cells, n 3 4 slices; spin-labeling: 109.2 3 57.6 nM, n 3 70 cells, n 3 3 slices; t-test, P 3 0.05). Finally, Ca23 responses elicited by bath application of the selective group I mGluR agonist (S)-3,5-dihydroxyphenylglycine (DHPG, 50 μM, 90 s) and by KCl depolarization (60 mM, 30 s) were undistinguishable (Fig. 1B). These results suggest that spin-labeling, compared with conventional bulk-labeling, does not change the basic Ca23 response properties of LSO neurons.

Developmental changes of group I mGluR-mediated Ca^{2+} responses

In LSO neurons from neonatal mice (P0–P5), Ca^{2+} responses elicited by DHPG (50 μM, 90 s) consisted of an initial peak followed by a large plateau phase that always exceeded the duration of the agonist application (Fig. 2). During post-natal development, these Ca^{2+} responses gradually changed their profile, amplitude, and duration (Fig. 2 and Table 1). At P9–P12, around hearing onset (approximately P10–P12; Shnerson and Pujol 1981;Song et al. 2006), peak and plateau amplitudes decreased and response durations had become shorter. By the end of the third postnatal week, plateau phases were absent in almost all responses. Response amplitudes, durations, and areas were significantly larger in the P0–P5 group compared with all older age groups (Mann–Whitney test, $P < 0.05$) and were significantly smaller in the P17–P19 group compared with all younger age groups (Mann–Whitney test, $P < 0.05$; Fig. 2*B* and Table 1; see also Supplemental Fig. S2).[1] Plateau amplitudes and response durations also signifi-cantly decreased from P9–P12 to P13–P16 (Mann–Whitney test, P 3 0.05; Fig. 2B and Table 1).

In the first postnatal week, all Ca^{2+} responses elicited by DHPG showed a prominent plateau and were categorized as pp responses ($n = 222/222$ cells, Fig. 2*C*). With increasing age, the frequency of pp responses decreased, from 100% at P0–P5 to 24% at P9–P12 ($n = 46/178$ cells), to 11% at P13–P16 ($n = 15/132$ cells) and to 7% at P17–P19 ($n = 4/54$ cells) (Fig. 2*C*). Responses with a peak and small plateau (psp responses) were found in all older age groups. The relative occurrence of responses that completely lacked a plateau (pnp responses) was age dependent as well, steadily increasing from 32% at P9–P12 ($n = 59/178$ cells), to 57% at P13–P16 ($n = 75/132$) and to 80% at P17–P19 ($n = 43/54$ cells).

In summary, during the first 3 week of postnatal development, group I mGluR-elicited Ca^{2+} responses gradually lose the sustained plateau phase that, in neonatal mice, is caused by an influx of extracellular Ca^{2+} through a channel not sensitive to voltage-gated calcium channel (VGCC) blockers (Ene et al. 2003). Next we used pharmacological tools to investigate the sources of $[Ca^{2+}]_i$ triggered by group I mGluRs in developing LSO neurons in more detail.

Contribution of extracellular Ca^{2+} to group I mGluR-elicited responses decreases during development

To determine the age dependency of mGluR-elicited influx of extracellular Ca^{2+} and its contribution to the three types of responses (pp, psp, pnp) we compared mGluR-elicited Ca^{2+} responses in standard and nominally Ca^{2+}-free ACSF (Fig. 3). Regardless of age, eliminating extracellular Ca^{2+} significantly reduced both the peak and the plateau phase of responses of the pp and psp type (P0–P5 pp response: peak reduced to 32 ± 2% and area to 13 ± 1%, $n = 82$; P9–P12 psp response: peak reduced to 23 ± 4% and area to 17 ± 4%, $n = 14$; P13–P16.psp response: Peak reduced to 44 ± 10% and area to 29 ± 6%, n 3 22). For pnp responses, however, removal of extracellular Ca^{2+} had no significant effect on response

[1]The online version of this article contains supplemental data.

amplitudes or areas (P13–P16 pnp response: peak reduced to 63 ± 11% and area to 80.9 ± 12.7%, $n = 19$; P17–P18 pnp response: peak reduced to 71 ± 12% and area to 88 ± 14%, $n = 16$). Thus in pp and psp responses extracellular Ca^{2+} influx accounted for 60–85% of the Ca^{2+} responses, whereas in pnp responses, extracellular Ca^{2+} contributed little (10–25%, statistically not significant). Finally, the hypothesis that mGluRs activate a membrane ion channel is supported by electrophysiological whole cell patch-clamp recordings from neonatal LSO neurons, demonstrating that DHPG elicits long-lasting membrane depolarizations (see Supplemental material).

In summary, during LSO development, the contribution of external Ca^{2+} influx to group I mGluR-elicited responses diminished progressively until it was absent in 3-wk-old mice, whereas the contribution of Ca^{2+} release from internal stores was present throughout the investigated period. We next investigated the pharmacological characteristics of the channel that mediates mGluR-elicited influx of extracellular Ca^{2+}.

mGluR-elicited extracellular Ca^{2+} influx is blocked by Ni^{2+}

In neonatal animals, short application of Ni^{2+} (2 mM for 2 min) during the plateau phase transiently abolished the response, indicating that the plateau is mediated by a Ni^{2+}-sensitive channel (Fig. 4*Ai*). Application of Ni^{2+} during the peak substantially decreased the peak amplitude to 14 ± 2% of its initial value ($n = 10$ cells, P5), indicating the contribution of Ni^{2+}-sensitive Ca^{2+} channels to the peak as well (Fig. 4*Aii*). In cells with pp and psp responses, DHPG application in the presence of Ni^{2+} only elicited small peak responses without plateaus (Fig. 4*A*, *iii–vi*). In contrast, in cells with pnp responses, Ni^{2+} had no effect (pnp responses, P13–P16: $n = 38$; P17–P18: $n = 23$) (Fig. 4, *Avii* and *Aviii*). This is consistent with our finding that extracellular Ca^{2+} contributes little, if any, to pnp responses (Fig. 3*B*). As a positive control, in cells with pnp responses, Ni^{2+} significantly reduced subsequent Ca^{2+} responses elicited by KCl depolarization (60 mM, 30 s) (66 ± 7% reduction at P13–P16, $n = 38$, and 80 ± 2% reduction at P17–P19, $n = 23$; *t*-test, $P < 0.05$).

In a small fraction of cells (P13–P16, $n = 7$ cells, $n = 3$ slices), Ni^{2+} potentiated the amplitude of pnp responses about fourfold (data not shown). It is possible that these cells represent a different population of LSO neurons (Ollo and Schwartz 1979), perhaps expressing different channel types.

DHPG-elicited Ca^{2+} responses are sensitive to 2-APB

In several neuron types, mGluRs can activate Ca^{2+}-permeable TRPCs (Bengtson et al. 2004; Kim et al. 2003; Tozzi et al. 2003). Because in LSO neurons, DHPG-elicited extracellular Ca^{2+} influx is independent of voltage-gated Ca^{2+} channels (Ene et al. 2003) but is blocked by Ni^{2+}, an unspecific blocker of TRPCs (Parekh et al. 1997), LSO neurons might express mGluR-activated TRPCs. To test this possibility, we used 2-aminoethoxydiphenyl borate (2-APB) that, in addition to its well-described function as a membrane-permeable inositol 1,4,5-triphosphate receptor (IP_3R) inhibitor, can act from the extracellular site to block TRPCs (Bootman et al. 2002; Ma et al. 2001; Maruyama et al. 1997).

At concentrations of 2–5 μM, 2-APB increased DHPG-elicited Ca^{2+} responses in LSO neurons (Fig. 5), consistent with what was reported in other neuronal and nonneuronal cells (Bootman et al. 2002;Prakriya and Lewis 2001;Tozzi et al. 2003). At concentrations of 10–50 μM, 2-APB reduced both peak and plateau amplitudes with the effect being more pronounced on the plateau phase, consistent with the hypothesis that TRPCs contribute more to the plateau phase than to the peak. Finally, at concentrations >50 μM, 2-APB completely abolished the response, most likely by inhibiting intracellular IP_3Rs and blocking Ca^{2+} release from intracellular stores, which is necessary to activate extracellular Ca^{2+} influx (Ene et al. 2003). Washout of 50 μM

2-APB for 30 min restored the peak component to 87 3 3%, whereas the plateau recovered to only 16 3 2% (n 3 65 cells). 2-APB did not reduce KCl-evoked Ca^{2+} responses (Fig. 5D), consistent with its reported lack of inhibiting VGCCs (Bootman et al. 2002;Maruyama et al. 1997) and further supporting our previous finding that mGluR-elicited influx of extracellular Ca^{2+} is independent of VGCCs (Ene et al. 2003).

Taken together, the sensitivity of DHPG-elicited Ca^{2+} response plateaus to Ni^{2+} and 2-APB and its insensitivity to specific VGCC blockers suggests that the plateau component is mediated by Ca^{2+} influx through a TRP-like channel.

DHPG responses are sensitive to La^{3+}

Most members of the TRPC family are either inhibited (TRPC3, TRPC6, and TRPC7 (Inoue et al. 2001; Okada et al. 1999; Zhu et al. 1998) or potentiated (TRPC4 and TRPC5; Schaefer et al. 2000; Strubing et al. 2001) by micromolar concentrations of La^{3+}. In neonatal LSO neurons (P0–P5), La^{3+} reduced DHPG responses in a dose-dependent manner and completely abolished them at 1 mM (Fig. 6*A*). La^{3+} at 1 mM also completely abolished KCl responses ($n = 49$ cells; data not shown), consistent with the known effect of La^{3+} on VGCCs (Ozawa et al. 1989). In P9–P12 animals, La^{3+}-potentiated responses at 0.1 and 0.5 mM but had no effect at 1 mM (Fig. 6, *B* and *C*). Sensitivity of DHPG-evoked responses to La^{3+} provides additional support that mGluR-evoked Ca^{2+} responses involve the activation of TRPCs. The age-dependent transition from inhibition to potentiation might be a consequence of an age-dependent expression of different TRPCs in LSO neurons.

Developmental downregulation of mGluR-mediated Ca^{2+} responses is impaired in deaf animals

The downregulation of group I mGluR-elicited Ca^{2+} responses and the disappearance of the plateau phase after hearing onset raises the question of whether these changes depend on auditory-evoked neuronal activity. To explore this idea, we compared DHPG-elicited Ca^{2+} responses from hearing wild-type (wt) C57/Bl mice to responses from age-matched deaf waltzer mice. In these experiments, we assessed hearing ability by the presence of a startle response to hand clapping. All wt mice older than P11 but none of the waltzer mice showed a clear startle response. LSO neurons from deaf waltzer mice showed DHPG-elicited Ca^{2+} responses of the pp, psp, and pnp types (Fig. 7*A*). Waltzer LSO neurons also showed an age-dependent decrease in peak amplitudes, areas, and duration of responses (P11–P16: $n = 107$ cells, P17–P20: 58 cells; Mann–Whitney test, $P < 0.05$). However, compared with age-matched wt mice, these changes were significantly different in waltzer mice (Fig. 7*B*). In both the P11–P16 group and the P17–P20 group, peak amplitudes were larger in waltzer mice than in age-matched wt mice (P11–P16: waltzer $n = 107$, wt $n = 68$; P17–P20: waltzer $n = 58$, wt $n = 72$; KS test, $P < 0.05$). This difference may be the result of a developmental delay because peak amplitudes from P17–P20 waltzer mice were not significantly different from those from P11–P16 wt mice (KS test, $P > 0.05$; Fig. 7*Bi*). Similarly, response durations were significantly larger in waltzer mice compared with aged-matched wt-mice (KS test, $P < 0.01$, Fig. 7*Bii*). However, response durations in P17–P20 waltzer mice were shorter than those in P11–P16 wt mice (KS test, $P < 0.01$).

We also investigated DHPG-elicited Ca^{2+} responses in heterozygote waltzer mice, which can hear but have elevated compound action potential thresholds and are more prone to noise-induced hearing loss (Holme and Steel 2004). The duration of DHPG-elicited Ca^{2+} responses in LSO neurons from hearing (startle positive) heterozygote mice ($n = 4$ animals) was the same as in neurons from hearing wt mice ($n = 11$ animals) (P11–P16: het mice $n = 44$, wt $n = 68$; P17–P20: het mice $n = 16$, wt $n = 72$; KS test, $P > 0.1$) (Fig. 8, *A* and *B*). At P11–P16, responses were significantly shorter in heterozygote mice compared with homozygote walzer mice ($n =$

6 animals; $n = 107$ cells, KS test, $P < 0.005$). In heterozygote mice, response durations in startle-negative P12–P13 mice were significantly longer compared with startle-positive P14–P16 mice (Fig. 8, *C* and *D*).

Similar to wt mice, in waltzer mice we also observed a developmental decrease in the percentage of DHPG-responses of the pp and psp types and a developmental increase in the percentage of pnp responses (Fig. 9; Fisher's exact test, $P < 0.05$). However, in waltzer mice, more cells showed pp and psp responses at P11–P16 (Fig. 9*A*; waltzer $n = 80$ cells, wt $n = 32$ cells; Fisher's exact test, $P < 0.05$).

Taken together, in deaf waltzer mice the age-dependent changes of mGluR-mediated Ca^{2+} responses were significantly smaller, suggesting that auditory experience is necessary for the normal time course of the functional downregulation of TRP-like channel(s). In support of this hypothesis, in P16 waltzer mice DHPG-elicited responses were strongly diminished by the TRPC antagonist Ni^{2+} (peak amplitude reduced by 80.5 ± 4.7%; area reduced by 82.4 ± 4.2%; $n = 21$ cells with responses in Ni^{2+}).

DISCUSSION

This study provides a developmental picture of the Ca^{2+} entry pathways underlying group I mGluR-mediated Ca^{2+} responses in developing LSO neurons. In neonatal mice, these Ca^{2+} responses were characterized by a large transient peak followed by a sustained plateau. We identified two Ca^{2+} sources that contributed to these responses: release of Ca^{2+} from internal stores and influx of Ca^{2+} from the extracellular milieu. The extracellular component was sensitive to the TRPC blockers Ni^{2+}, 2-APB, and La^{3+}, suggesting that it was mediated by a TRP-like Ca^{2+} channel. With increasing age, the contribution of extracellular Ca^{2+} influx to group I mGluR-mediated Ca^{2+} responses diminished and was mostly absent after hearing onset, whereas the contribution of internal stores was unchanged. Finally, the developmental downregulation of mGluR-elicited extracellular Ca^{2+} influx was delayed in deaf waltzer mice, suggesting that an age-dependent decrease in the activation and/or expression of TRPCs is influenced by auditory experience.

Developing LSO neurons express functional TRP-like channels

Our results suggest that LSO neurons in prehearing mice express Ca^{2+}-permeable, TRP-like channels that are activated by group I mGluRs. This is supported by the following observations. First, the typical biphasic peak-plateau profile of mGluR-elicited Ca^{2+} responses in LSO neurons resembles the response profiles that were observed in a number of other neuronal and nonneuronal cell types that express store-operated Ca^{2+} channels or TRPCs (Boulay et al. 1997; Hu et al. 1994; Moller et al. 1997; Ramsey et al. 2006; Sosa et al. 2002). Second, the plateau phase of mGluR-elicted Ca^{2+} responses was mediated entirely by influx of extracellular Ca^{2+} (Ene et al. 2003). Third, extracellular Ca^{2+} influx was insensitive to specific blockers of voltage-gated Ca^{2+} channels (Ene et al. 2003) but was sensitive to blockers of TRPCs such as Ni^{2+}, 2-APB, and La^{3+} (Figs. 4–6). Fourth, activation of mGluRs by the specific agonist DHPG resulted in depolarizations (see Supplemental material) similar to the activation of TRPCs in other neuronal systems (Kim et al. 2003. Tempia et al. 2001).

TRPCs can be activated by a variety of intracellular messengers depending on the exact TRPC and cell type. In LSO neurons, Ca^{2+} release from intracellular Ca^{2+} stores is required for coupling mGluR activation to the opening of TRP-like channels—based on the observation that depletion of intracellular Ca^{2+} stores with thapsigargine abolished all mGluR-elicited Ca^{2+} responses (Ene et al. 2003). However, Ca^{2+} does not appear to be the only signal responsible for activation of TRP-like channels because influx of Ca^{2+} through VGCC while intracellular Ca^{2+} stores were depleted by thapsigargine did not trigger long-lasting Ca^{2+}

plateaus. Further studies are needed to identify what additional components of the group I mGluR-activated intracellular cascade are the relevant stimuli that, together with Ca^{2+}, activate the opening of TRP-like channels in LSO neurons.

Which TRPCs are responsible for group I mGluR-mediated Ca^{2+} responses in LSO neurons? All members of the TRPC family (TRPC1–TRPC7) are expressed in the brain (Minke and Cook 2002; Riccio et al. 2002), although their expression patterns have not been investigated specifically for the LSO. TRPCs are activated by an increase in $[Ca^{2+}]_i$ and/or diacyl-glycerol (Boulay et al. 1997; Hofmann et al. 1999; Kim et al. 2003; Okada et al. 1998; Schaefer et al. 2000; Zitt et al. 1997) and it was previously suggested that the TRPC3 channel mediates group I mGluR-mediated Ca^{2+} responses in retinal amacrine cells (Sosa et al. 2002). TRPC3 also seems to be a good candidate for LSO neurons because TRPC3 is strongly expressed in the embryonic and early postnatal brain stem, including in auditory brain stem nuclei (Li et al. 1999), and because TRPC3 expression levels decrease after P10, which corresponds to the time when group I mGluR-mediated Ca^{2+} responses in LSO neurons also decrease. Finally, DHPG-evoked responses in neonatal LSO neurons were inhibited by millimolar concentrations of La^{3+} (Fig. 6), concentrations that are in the range of TRPC3 sensitivity to La^{3+} (Zhu et al. 1998).

Developmental decrease in the contribution of TRP-like channels to mGluR-mediated Ca^{2+} responses and the role of sensory-evoked activity

During the first three postnatal weeks, group I mGluR-mediated Ca^{2+} responses became progressively smaller in amplitude, shorter in duration, and the plateau component disappeared (Fig. 2). These changes are consistent with the idea that the decrease in mGluR-elicited Ca^{2+} responses resulted, in large part, from a developmental downregulation of TRP-like channels or their functional uncoupling from mGluR activation. In support of this, both Ni^{2+}, which reduced the peak amplitude and abolished the Ca^{2+} plateau by blocking the influx of extracellular Ca^{2+} in neonatal LSO neurons, and removal of extracellular Ca^{2+} (Fig. 3) had no effect on responses during the third postnatal week, when most responses were small and short and were mediated primarily by Ca^{2+} release from internal stores (Fig. 4, *A* and *B*).

The contribution of extracellular Ca^{2+} influx to mGluR-mediated Ca^{2+} responses declined at, and shortly after, hearing onset (approximately P12; Song et al. 2006), raising the possibility that sensory activity plays a role in the functional downregulation of TRP-like channels. We tested this hypothesis by investigating mGluR-mediated Ca^{2+} responses in developing waltzer mice. Waltzer mice have spontaneous mutation in the gene for cadherin 23, which causes a disorganization of stereocilia bundles of cochlear hair cells resulting in deafness (Di Palma et al. 2001; Holme and Steel 2002). In waltzer mice, the changes in group I mGluR-mediated Ca^{2+} responses appeared to be significantly delayed compared with heterozygote and wild-type control mice (Figs. 7–9). Notably, more LSO neurons in waltzer mice than in age-matched control mice displayed responses with a long Ca^{2+} plateau and fewer neurons displayed peak-only responses. These results support the idea that auditory experience is important for the developmental downregulation of TRP-like channel expression or their developmental uncoupling from mGluR activation.

It should be noted that our results cannot exclude the possibility that spontaneous activity before hearing onset also contributes to the downregulation of TRP-like responses. Further studies that investigate mGluR-mediated Ca^{2+} responses in prehearing waltzer mice and characterize spontaneous activity patterns in vivo are necessary to conclusively address this possibility. Another issue to consider is that cadherin 23 is expressed not only in hair cells but also in the brain (Di Palma 2001; Rzadzinska et al. 2005), although it is currently unknown whether cadherin 23 is expressed in the LSO or in any other auditory nuclei. Anatomical studies investigating cadherin expression in developing LSO neurons are required to address the

question whether impairment in the developmental decrease in TRP-like channels activation by mGluRs in waltzer mice is influenced by potential changes of cadherin 23 in the LSO. Nevertheless, our conclusion that auditory experience is an important contributing factor to the downregulation of TRP activation by mGluRs is supported by our results from heterozygote waltzer mice. Heterozygotes, after hearing onset, as indicated by the presence of an acoustic startle response, showed mGluR-mediated Ca^{2+} responses similar to age-matched wild-type mice and in P12–P16 heterozygotes response durations became significantly shorter right after hearing onset (Fig. 8, *C* and *D*).

Functional implications

Similar to other neuronal types, in neonatal LSO neurons mGluRs are activated preferentially by high-frequency stimulation of glutamatergic inputs (Ene et al. 2003). Spontaneous high-frequency bursts of neuronal activity exist in a variety of auditory nuclei before hearing onset (Durham et al. 1989; Gummer and Mark 1994; Jones et al. 2001; Kotak and Sanes 1995; Kros et al. 1998; Leao et al. 2006; Lippe 1994), making it likely that TRP-like channels in LSO neurons are activated by spontaneous burstlike activity in vivo. In addition to LSO neurons, opening of TRPCs by mGluR activation also seems to occur in other auditory brain stem neurons. For example, in neonatal rat MNTB neurons, DHPG elicits inward currents (Kushmerick et al. 2004) and in preliminary studies we observed long-lasting Ca^{2+} responses with typical peak-plateau profiles after DHPG application in the MNTB.

Spontaneous activity before hearing onset is important for numerous developmental processes including neuronal survival of auditory brain stem neurons (Sie and Rubel 1992; Zirpel and Rubel 1996) and various other aspects of auditory brain stem circuits (Gabriele et al. 2000; Kitzes et al. 1995; Kotak and Sanes 1997; Russell and Moore 1995; Sanes and Takacs 1993). Intracellular Ca^{2+} plays a central role in linking neuronal activity to the survival of auditory brain stem neurons (Lachica et al. 1995; Lohmann et al. 1998; Zirpel et al. 1995) and was previously implicated in activity-dependent refinement of LSO circuitry (Kotak and Sanes 2000). TRP-like channels, by greatly amplifying the initial mGluR-elicited Ca^{2+} response (Figs. 3 and 4), may provide an important function in translating burstlike synaptic activity into functional LSO circuitry, perhaps by influencing growth cone behavior (Li et al. 2005; Wang and Poo 2005), regulating neurite length (Greka et al. 2003), or by adjusting synaptic strength (Baba et al. 2003). In the LSO, TRP-like channels are activated preferentially before hearing onset, which is the period of major developmental changes that include dendritic and synaptic refinement (Kim and Kandler 2003; Rietzel and Friauf 1998; Sanes and Takacs 1993; Sanes et al. 1992), activity-dependent plasticity (Kotak and Sanes 2000), and a switch of neurotransmitter phenotype (Gillespie et al. 2005; Kotak et al. 1998; Nabekura et al. 2004).

It will be interesting to find out whether and to what degree mGluR activation and TRPCs are involved in mediating any or which of these events and thus contribute to the development of normal sound localization and hearing.

Although activation of TRPCs by mGluRs might play an important role in the cellular detection and encoding of spontaneous bursts of activity, auditory experience-dependent downregulation of TRPC activation might protect LSO neurons from reaching toxic levels of $[Ca^{2+}]_i$ after hearing onset when glutamatergic inputs to LSO neurons fire at high rates and when LSO neurons express Ca^{2+}-permeable μ-amino-3-hydroxy-5-methyl-4-isoxazolepropionic acid (AMPA) receptors (Caicedo et al. 1998).

Finally, TRPCs might plausibly be the mechanism responsible for long-lasting depolarizations that occur in LSO neurons of neonatal gerbils after tetanic stimulation of glutama-tergic cochlea nucleus afferents (Kotak and Sanes 1995). These long-lasting depolarizations occur during the

first two postnatal weeks, require mGluR receptors activation, and are sensitive to Ni^{2+}, properties that parallel mGluR-mediated TRPC activation.

Supplementary Material

Refer to Web version on PubMed Central for supplementary material.

Acknowledgements

We thank K. Cihil for excellent technical support, D. Goldring for editorial help, NBK for encouragement, and Dr. Elias Aizenman and members of the Kandler laboratory for valuable discussion.

GRANTS

This work was supported by National Institute on Deafness and Other Communication Disorders Grants DC-04199 and DC-008938 to K. Kandler and A. Kalmbach, respectively, and by the Center for the Neural Basis of Cognition at Carnegie Mellon University and the University of Pittsburgh.

References

Baba A, Yasui T, Fujisawa S, Yamada RX, Yamada MK, Nishiyama N, Matsuki N, Ikegaya Y. Activity-evoked capacitative Ca^{2+} entry: implications in synaptic plasticity. J Neurosci 2003;23:7737–7741. [PubMed: 12944501]

Bengtson CP, Tozzi A, Bernardi G, Mercuri NB. Transient receptor potential-like channels mediate metabotropic glutamate receptor EPSCs in rat dopamine neurones. J Physiol 2004;555:323–330. [PubMed: 14724196]

Bootman MD, Collins TJ, Mackenzie L, Roderick HL, Berridge MJ, Peppiatt CM. 2-Aminoethoxydiphenyl borate (2-APB) is a reliable blocker of store-operated Ca^{2+} entry but an inconsistent inhibitor of InsP3-induced Ca^{2+} release. FASEB J 2002;16:1145–1150. [PubMed: 12153982]

Boudreau JC, Tsuchitani C. Binaural interaction in the cat superior olive S segment. J Neurophysiol 1968;31:442–454. [PubMed: 5687764]

Boulay G, Zhu X, Peyton M, Jiang M, Hurst R, Stefani E, Birnbaumer L. Cloning and expression of a novel mammalian homolog of Drosophila transient receptor potential (Trp) involved in calcium entry secondary to activation of receptors coupled by the Gq class of G protein. J Biol Chem 1997;272:29672–29680. [PubMed: 9368034]

Caicedo A, Kungel M, Pujol R, Friauf E. Glutamate-induced Co^{2+} uptake in rat auditory brainstem neurons reveals developmental changes in Ca^{2+} permeability of glutamate receptors. Eur J Neurosci 1998;10:941–954. [PubMed: 9753161]

Clapham DE. TRP channels as cellular sensors. Nature 2003;426:517–524. [PubMed: 14654832]

Di Palma F, Holme RH, Bryda EC, Belyantseva IA, Pellegrino R, Kachar B, Steel KP, Noben-Trauth K. Mutations in Cdh23, encoding a new type of cadherin, cause stereocilia disorganization in waltzer, the mouse model for Usher syndrome type 1D. Nat Genet 2001;27:103–107. [PubMed: 11138008]

Durham D, Rubel EW, Steel KP. Cochlear ablation in deafness mutant mice: 2-eoxyglucose analysis suggests no spontaneous activity of cochlear origin. Hear Res 1989;43:39–46. [PubMed: 2613565]

Ene FA, Kullmann PH, Gillespie DC, Kandler K. Glutamatergic calcium responses in the developing lateral superior olive: receptor types and their specific activation by synaptic activity patterns. J Neurophysiol 2003;90:2581–2591. [PubMed: 12853437]

Friauf E, Lohmann C. Development of auditory brainstem circuitry. Activity-dependent and activity-independent processes. Cell Tissue Res 1999;297:187–195. [PubMed: 10470488]

Gabriele ML, Brunso-Bechtold JK, Henkel CK. Plasticity in the development of afferent patterns in the inferior colliculus of the rat after unilateral cochlear ablation. J Neurosci 2000;20:6939–6949. [PubMed: 10995838]

Gee CE, Benquet P, Gerber U. Group I metabotropic glutamate receptors activate a calcium-sensitive transient receptor potential-like conductance in rat hippocampus. J Physiol 2003;546:655–664. [PubMed: 12562994]

Gillespie DC, Kim G, Kandler K. Inhibitory synapses in the developing auditory system are glutamatergic. Nat Neurosci 2005;8:332–338. [PubMed: 15746915]

Glowatzki E, Fuchs PA. Cholinergic synaptic inhibition of inner hair cells in the neonatal mammalian cochlea. Science 2000;288:2366–2368. [PubMed: 10875922]

Greka A, Navarro B, Oancea E, Duggan A, Clapham DE. TRPC5 is a regulator of hippocampal neurite length and growth cone morphology. Nat Neurosci 2003;6:837–845. [PubMed: 12858178]

Grynkiewicz G, Poenie M, Tsien RY. A new generation of Ca^{2+} indicators with greatly improved fluorescence properties. J Biol Chem 1985;260:3440–3450. [PubMed: 3838314]

Gummer AW, Mark RF. Patterned neural activity in brain stem auditory areas of a prehearing mammal, the tammar wallaby (*Macropus eugenii*). Neuroreport 1994;5:685–688. [PubMed: 8199338]

Hofmann T, Obukhov AG, Schaefer M, Harteneck C, Gudermann T, Schultz G. Direct activation of human TRPC6 and TRPC3 channels by diacylglycerol. Nature 1999;397:259–263. [PubMed: 9930701]

Holme RH, Steel KP. Stereocilia defects in waltzer (Cdh23), shaker1 (Myo7a) and double waltzer/shaker1 mutant mice. Hear Res 2002;169:13–23. [PubMed: 12121736]

Holme RH, Steel KP. Progressive hearing loss and increased susceptibility to noise-induced hearing loss in mice carrying a Cdh23 but not a Myo7a mutation. J Assoc Res Otolaryngol 2004;5:66–79. [PubMed: 14648237]

Hu Y, Vaca L, Zhu X, Birnbaumer L, Kunze DL, Schilling WP. Appearance of a novel Ca^{2+} influx pathway in Sf9 insect cells following expression of the transient receptor potential-like (trpl) protein of Drosophila. Biochem Biophys Res Commun 1994;201:1050–1056. [PubMed: 7516156]

Inoue R, Okada T, Onoue H, Hara Y, Shimizu S, Naitoh S, Ito Y, Mori Y. The transient receptor potential protein homologue TRP6 is the essential component of vascular alpha(1)-adrenoceptor-activated Ca (2+)-permeable cation channel. Circ Res 2001;88:325–332. [PubMed: 11179201]

Jones TA, Jones SM, Paggett KC. Primordial rhythmic bursting in embryonic cochlear ganglion cells. J Neurosci 2001;21:8129–8135. [PubMed: 11588185]

Kandler K, Gillespie DC. Developmental refinement of inhibitory sound-localization circuits. Trends Neurosci 2005;28:290–296. [PubMed: 15927684]

Kim G, Kandler K. Elimination and strengthening of glycinergic/GABAergic connections during tonotopic map formation. Nat Neurosci 2003;6:282–290. [PubMed: 12577063]

Kim SJ, Kim YS, Yuan JP, Petralia RS, Worley PF, Linden DJ. Activation of the TRPC1 cation channel by metabotropic glutamate receptor mGluR1. Nature 2003;426:285–291. [PubMed: 14614461]

Kitzes LM, Kageyama GH, Semple MN, Kil J. Development of ectopic projections from the ventral cochlear nucleus to the superior olivary complex induced by neonatal ablation of the contralateral cochlea. J Comp Neurol 1995;353:341–363. [PubMed: 7751435]

Kotak VC, Korada S, Schwartz IR, Sanes DH. A developmental shift from GABAergic to glycinergic transmission in the central auditory system. J Neurosci 1998;18:4646–4655. [PubMed: 9614239]

Kotak VC, Sanes DH. Synaptically evoked prolonged depolarizations in the developing auditory system. J Neurophysiol 1995;74:1611–1620. [PubMed: 8989397]

Kotak VC, Sanes DH. Deafferentation weakens excitatory synapses in the developing central auditory system. Eur J Neurosci 1997;9:2340–2347. [PubMed: 9464928]

Kotak VC, Sanes DH. Long-lasting inhibitory synaptic depression is age- and calcium-dependent. J Neurosci 2000;20:5820–5826. [PubMed: 10908623]

Kros CJ, Ruppersberg JP, Rusch A. Expression of a potassium current in inner hair cells during development of hearing in mice. Nature 1998;394:281–284. [PubMed: 9685158]

Kushmerick C, Price GD, Taschenberger H, Puente N, Renden R, Wadiche JI, Duvoisin RM, Grandes P, von Gersdorff H. Retroinhibition of presynaptic Ca^{2+} currents by endocannabinoids released via postsynaptic mGluR activation at a calyx synapse. J Neurosci 2004;24:5955–5965. [PubMed: 15229243]

Lachica EA, Rubsamen R, Zirpel L, Rubel EW. Glutamatergic inhibition of voltage-operated calcium channels in the avian cochlear nucleus. J Neurosci 1995;15:1724–1734. [PubMed: 7891130]

Leao RN, Sun H, Svahn K, Berntson A, Youssoufian M, Paolini AG, Fyffe RE, Walmsley B. Topographic organization in the auditory brainstem of juvenile mice is disrupted in congenital deafness. J Physiol 2006;571:563–578. [PubMed: 16373385]

Li HS, Xu XZ, Montell C. Activation of a TRPC3-dependent cation current through the neurotrophin BDNF. Neuron 1999;24:261–273. [PubMed: 10677043]

Li Y, Jia YC, Cui K, Li N, Zheng ZY, Wang YZ, Yuan XB. Essential role of TRPC channels in the guidance of nerve growth cones by brain-derived neurotrophic factor. Nature 2005;434:894–898. [PubMed: 15758952]

Lippe WR. Rhythmic spontaneous activity in the developing avian auditory system. J Neurosci 1994;14:1486–1495. [PubMed: 8126550]

Lohmann C, Ilic V, Friauf E. Development of a topographically organized auditory network in slice culture is calcium dependent. J Neurobiol 1998;34:97–112. [PubMed: 9468382]

Ma HT, Venkatachalam K, Li HS, Montell C, Kurosaki T, Patterson RL, Gill DL. Assessment of the role of the inositol 1,4,5-trisphosphate receptor in the activation of transient receptor potential channels and store-operated Ca^{2+} entry channels. J Biol Chem 2001;276:18888–18896. [PubMed: 11259416]

Maruyama T, Kanaji T, Nakade S, Kanno T, Mikoshiba K. 2APB, 2-aminoethoxydiphenyl borate, a membrane-penetrable modulator of Ins(1,4,5)P3-induced Ca^{2+} release. J Biochem (Tokyo) 1997;122:498–505. [PubMed: 9348075]

Minke B, Cook B. TRP channel proteins and signal transduction. Physiol Rev 2002;82:429–472. [PubMed: 11917094]

Moller T, Nolte C, Burger R, Verkhratsky A, Kettenmann H. Mechanisms of C5a and C3a complement fragment-induced $[Ca^{2+}]_i$ signaling in mouse microglia. J Neurosci 1997;17:615–624. [PubMed: 8987784]

Montell C. TRP channels in Drosophila photoreceptor cells. J Physiol 2005;567:45–51. [PubMed: 15961416]

Nabekura J, Katsurabayashi S, Kakazu Y, Shibata S, Matsubara A, Jinno S, Mizoguchi Y, Sasaki A, Ishibashi H. Developmental switch from GABA to glycine release in single central synaptic terminals. Nat Neurosci 2004;7:17–23. [PubMed: 14699415]

Oertel D. The role of timing in the brain stem auditory nuclei of vertebrates. Annu Rev Physiol 1999;61:497–519. [PubMed: 10099699]

Okada T, Inoue R, Yamazaki K, Maeda A, Kurosaki T, Yamakuni T, Tanaka I, Shimizu S, Ikenaka K, Imoto K, Mori Y. Molecular and functional characterization of a novel mouse transient receptor potential protein homologue TRP7. Ca(2+)-permeable cation channel that is constitutively activated and enhanced by stimulation of G protein-coupled receptor. J Biol Chem 1999;274:27359–27370. [PubMed: 10488066]

Okada T, Shimizu S, Wakamori M, Maeda A, Kurosaki T, Takada N, Imoto K, Mori Y. Molecular cloning and functional characterization of a novel receptor-activated TRP Ca^{2+} channel from mouse brain. J Biol Chem 1998;273:10279–10287. [PubMed: 9553080]

Ollo C, Schwartz IR. The superior olivary complex in C57BL/6 mice. Am J Anat 1979;155:349–374. [PubMed: 474450]

Ozawa S, Tsuzuki K, Iino M, Ogura A, Kudo Y. Three types of voltage-dependent calcium current in cultured rat hippocampal neurons. Brain Res 1989;495:329–336. [PubMed: 2548673]

Parekh AB, Fleig A, Penner R. The store-operated calcium current I(CRAC): nonlinear activation by InsP3 and dissociation from calcium release. Cell 1997;89:973–980. [PubMed: 9200615]

Prakriya M, Lewis RS. Potentiation and inhibition of Ca(2+) release-activated Ca(2+) channels by 2-aminoethyldiphenyl borate (2-APB) occurs independently of IP(3) receptors. J Physiol 2001;536:3–19. [PubMed: 11579153]

Ramsey IS, Delling M, Clapham DE. An introduction to trp channels. Annu Rev Physiol 2006;68:619–647. [PubMed: 16460286]

Riccio A, Mattei C, Kelsell RE, Medhurst AD, Calver AR, Randall AD, Davis JB, Benham CD, Pangalos MN. Cloning and functional expression of human short TRP7, a candidate protein for store-operated Ca^{2+} influx. J Biol Chem 2002;277:12302–12309. [PubMed: 11805119]

Rietzel HJ, Friauf E. Neuron types in the rat lateral superior olive and developmental changes in the complexity of their dendritic arbors. J Comp Neurol 1998;390:20–40. [PubMed: 9456173]

Romand R, Ehret G. Development of tonotopy in the inferior colliculus. I. Electrophysiological mapping in house mice. Dev Brain Res 1990;54:221–234. [PubMed: 2397588]

Russell FA, Moore DR. Afferent reorganisation within the superior olivary complex of the gerbil: development and induction by neonatal, unilateral cochlear removal. J Comp Neurol 1995;352:607–625. [PubMed: 7722003]

Rzadzinska AK, Derr A, Kachar B, Noben-Trauth K. Sustained cadherin 23 expression in young and adult cochlea of normal and hearing-impaired mice. Hear Res 2005;208:114–121. [PubMed: 16005171]

Sanes DH, Rubel EW. The ontogeny of inhibition and excitation in the gerbil lateral superior olive. J Neurosci 1988;8:682–700. [PubMed: 3339433]

Sanes DH, Siverls V. Development and specificity of inhibitory terminal arborizations in the central nervous system. J Neurobiol 1991;8:837–854. [PubMed: 1663990]

Sanes DH, Song J, Tyson J. Refinement of dendritic arbors along the tonotopic axis of the gerbil lateral superior olive. Dev Brain Res 1992;67:47–55. [PubMed: 1638742]

Sanes DH, Takacs C. Activity-dependent refinement of inhibitory connections. Eur J Neurosci 1993;5:570–574. [PubMed: 8261131]

Schaefer M, Plant TD, Obukhov AG, Hofmann T, Gudermann T, Schultz G. Receptor-mediated regulation of the nonselective cation channels TRPC4 and TRPC5. J Biol Chem 2000;275:17517–17526. [PubMed: 10837492]

Scheenen WJ, Makings LR, Gross LR, Pozzan T, Tsien RY. Photodegra-dation of indo-1 and its effect on apparent Ca^{2+} concentrations. Chem Biol 1996;3:765–774. [PubMed: 8939693]

Shnerson A, Pujol R. Age-related changes in the C57BL/6J mouse cochlea. I. Physiological findings. Brain Res 1981;254:65–75. [PubMed: 7272773]

Sie KC, Rubel EW. Rapid changes in protein synthesis and cell size in the cochlear nucleus following eighth nerve activity blockade or cochlea ablation. J Comp Neurol 1992;320:501–508. [PubMed: 1629400]

Song L, Mcgee J, Walsh EJ. Frequency- and level-dependent changes in auditory brainstem responses (ABRS) in developing mice. J Acoust Soc Am 2006;119:2242–2257. [PubMed: 16642839]

Sosa R, Hoffpauir B, Rankin ML, Bruch RC, Gleason EL. Metabotropic glutamate receptor 5 and calcium signaling in retinal amacrine cells. J Neu-rochem 2002;81:973–983.

Strubing C, Krapivinsky G, Krapivinsky L, Clapham DE. TRPC1 and TRPC5 form a novel cation channel in mammalian brain. Neuron 2001;29:645–655. [PubMed: 11301024]

Tempia F, Alojado ME, Strata P, Knopfel T. Characterization of the mGluR(1)-mediated electrical and calcium signaling in Purkinje cells of mouse cerebellar slices. J Neurophysiol 2001;86:1389–1397. [PubMed: 11535685]

Tollin DJ. The lateral superior olive: a functional role in sound source localization. Neuroscientist 2003;9:127–143. [PubMed: 12708617]

Tozzi A, Bengtson CP, Longone P, Carignani C, Fusco FR, Bernardi G, Mercuri NB. Involvement of transient receptor potential-like channels in responses to mGluR-I activation in midbrain dopamine neurons. Eur J Neu-rosci 2003;18:2133–2145.

Wada T, Wakabayashi Y, Takahashi S, Ushiki T, Kikkawa Y, Yonekawa H, Kominami R. A point mutation in a cadherin gene, Cdh23, causes deafness in a novel mutant, Waltzer mouse niigata. Biochem Biophys Res Commun 2001;283:113–117. [PubMed: 11322776]

Wang GX, Poo MM. Requirement of TRPC channels in netrin-1-induced chemotropic turning of nerve growth cones. Nature 2005;434:898–904. [PubMed: 15758951]

Zhu X, Jiang M, Birnbaumer L. Receptor-activated Ca^{2+} influx via human Trp3 stably expressed in human embryonic kidney (HEK)293 cells. Evidence for a non-capacitative Ca^{2+} entry. J Biol Chem 1998;273:133–142. [PubMed: 9417057]

Zirpel L, Lachica EA, Rubel EW. Activation of a metabotropic glutamate receptor increases intracellular calcium concentrations in neurons of the avian cochlear nucleus. J Neurosci 1995;15:214–222. [PubMed: 7823131]

Zirpel L, Rubel EW. Eighth nerve activity regulates intracellular calcium concentration of avian cochlear nucleus neurons via a metabotropic glutamate receptor. J Neurophysiol 1996;76:4127–4139. [PubMed: 8985906]

Zitt C, Obukhov AG, Strubing C, Zobel A, Kalkbrenner F, Luckhoff A, Schultz G. Expression of TRPC3 in Chinese hamster ovary cells results in calcium-activated cation currents not related to store depletion. J Cell Biol 1997;138:1333–1341. [PubMed: 9298988]

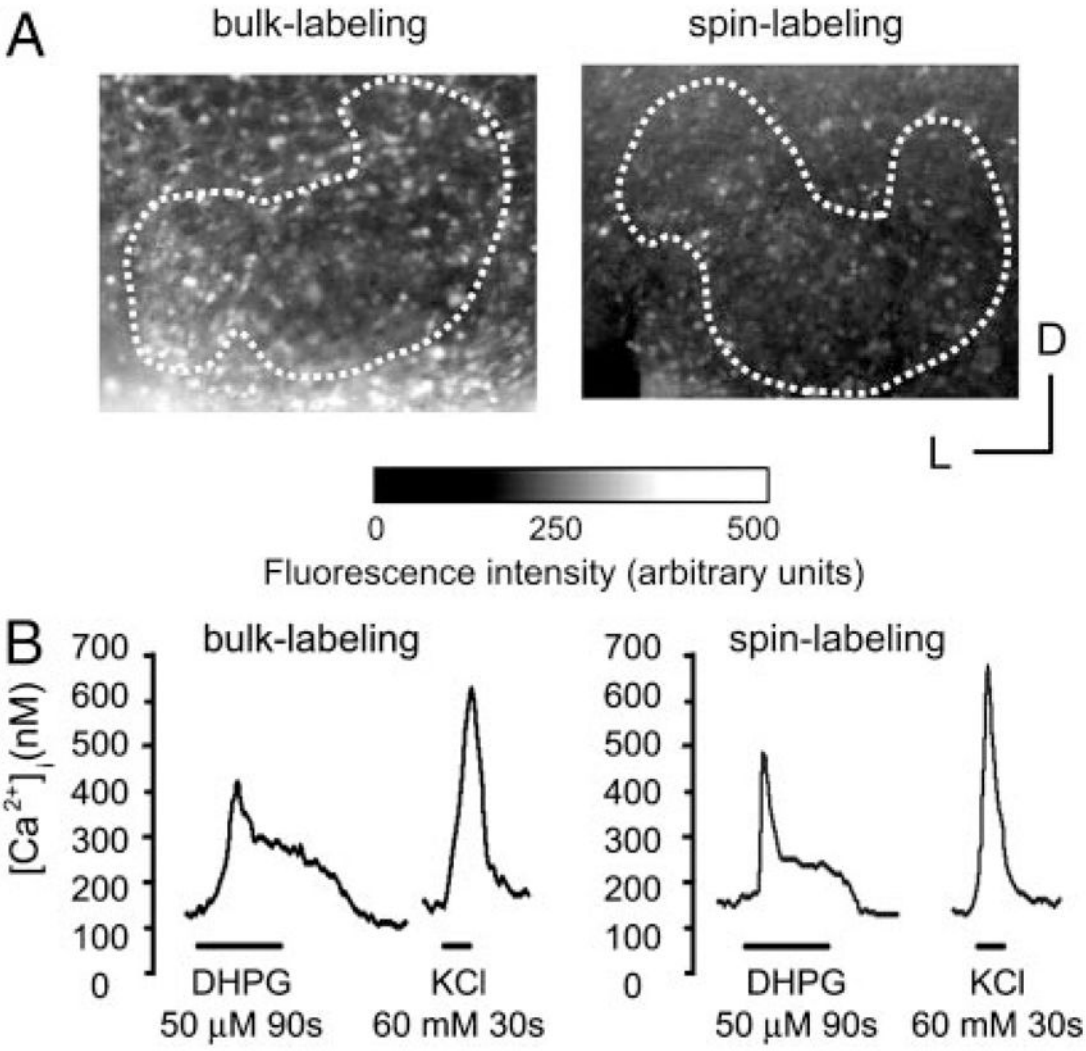

FIG. 1.

Comparisons between bulk-labeling and spin-labeling. *A*: examples of lateral superior olive (LSO) slices labeled using bulk (*left*) and spin-labeling (*right*) at postnatal day 0 (P0: the day of birth). Images show fluorescence at 360 nm (exposure time 20 ms, ×20 objective). Dotted lines outline the boundaries of the LSO. D, dorsal; L, lateral. *B*: example of changes in intracellular Ca^{2+} elicited by bath application of (*S*)-3,5-dihydroxyphenylglycine (DHPG, 50 μM, 90 s) and KCl (60 mM, 30 s). LSO neurons from a P3-old mouse.

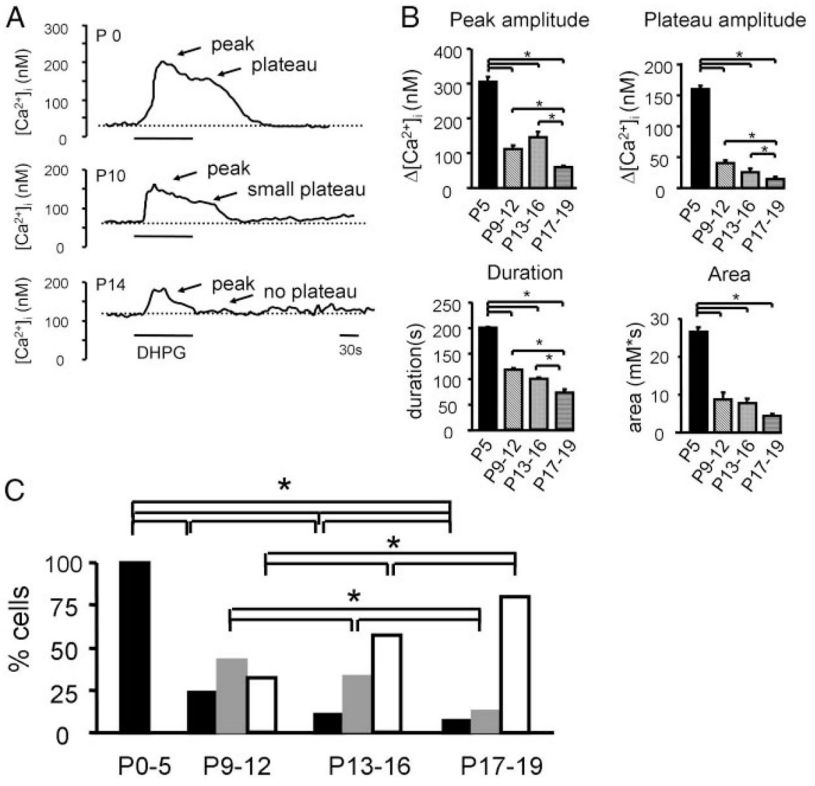

FIG. 2.

Developmental changes of group I metabo-tropic glutamate receptor (mGluR)–mediated Ca^{2+} responses in LSO neurons. *A*: example of DHPG-elicited (50 μM, 90 s) Ca^{2+} responses in 3 LSO neurons, each from a P0, P10, and P14 mouse. Responses undergo a transition from a profile characterized by peak and plateau (pp) to a profile characterized by a smaller peak and a smaller plateau (psp), and finally to a profile characterized by a peak only [peak and no plateau (pnp)]. Dotted line indicates baseline Ca^{2+} levels. *B*: group data of peak amplitudes, plateau amplitudes, area, and duration of DHPG-evoked Ca^{2+} responses at different ages. Number of cells in each age group: P0–P5: 222; P9–P12: 165; P13–P16: 135; P17–P19: 54 (asterisks: $P < 0.05$, ANOVA). *C*: developmental changes in the percentage of pp-type (black bars), psp-type (gray bars), and pnp-type (white bars) responses (asterisks: $P < 0.05$, chi-square test). Number of cells in each age group: P0–P5: pp $n = 222$; P9–P12: pp $n = 46$; psp $n = 75$, pnp $n = 59$; P13–P16: pp $n = 15$, psp $n = 42$, pnp $n = 75$; P17–P19: pp $n = 4$, psp $n = 7$, pnp $n = 43$.

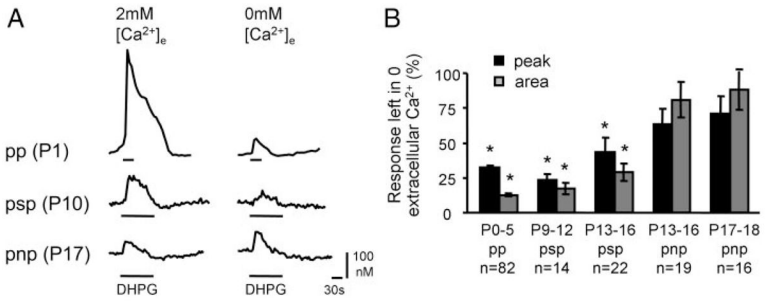

FIG. 3.

Developmental changes in the contribution of extracellular Ca^{2+} to group I mGluR-mediated Ca^{2+} responses. *A*: examples of individual responses to DHPG application in 2 mM extracellular Ca^{2+} (*left traces*) and in 0 mM Ca^{2+} (*right traces*). *B*: peak and area of Ca^{2+} responses after removal of extracellular Ca^{2+} as a function of age and response type. *n*, number of cells. Asterisks: $P < 0.05$ (paired *t*-test)

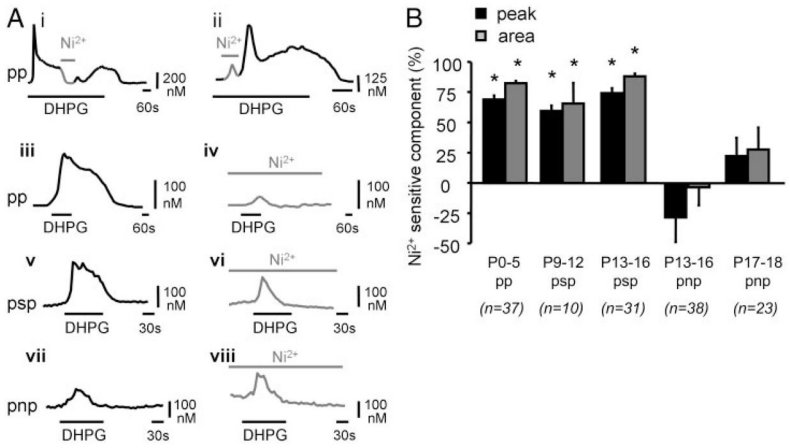

FIG. 4.

Effect of Ni^{2+} on mGluR-mediated Ca^{2+} responses. *A*: examples of DHPG-elicited (20–50 μM) Ca^{2+} responses from individual LSO neurons. *Ai*: short application of Ni^{2+} (2 mM, 2 min) during the plateau phase reduces the response to baseline. *Aii*: application of Ni^{2+} (2 mM, 2 min) together with DHPG reduces the amplitude of the initial peak response. Example is from a P5 neuron. *Aiii–Avi*: DHPG-elicited (50 μM, 90 s) responses of the pp and psp type (*iii* and *v*) are reduced by Ni^{2+} (2 mM). Plateau phase is completely abolished and the peak phase is substantially reduced. Examples are from a P2 (pp response) and a P10 mouse (psp response). *Avii–Aviii*: DHPG-elicited (50 μM, 90 s) responses of the pnp type are unaffected by Ni^{2+} (2 mM). Example is from a P15 mouse. *B*: summary of the effects of Ni^{2+} on DHPG-elicited Ca^{2+} responses. Asterisks: sig-nificantly different from control ($P < 0.05$, paired *t*-test).

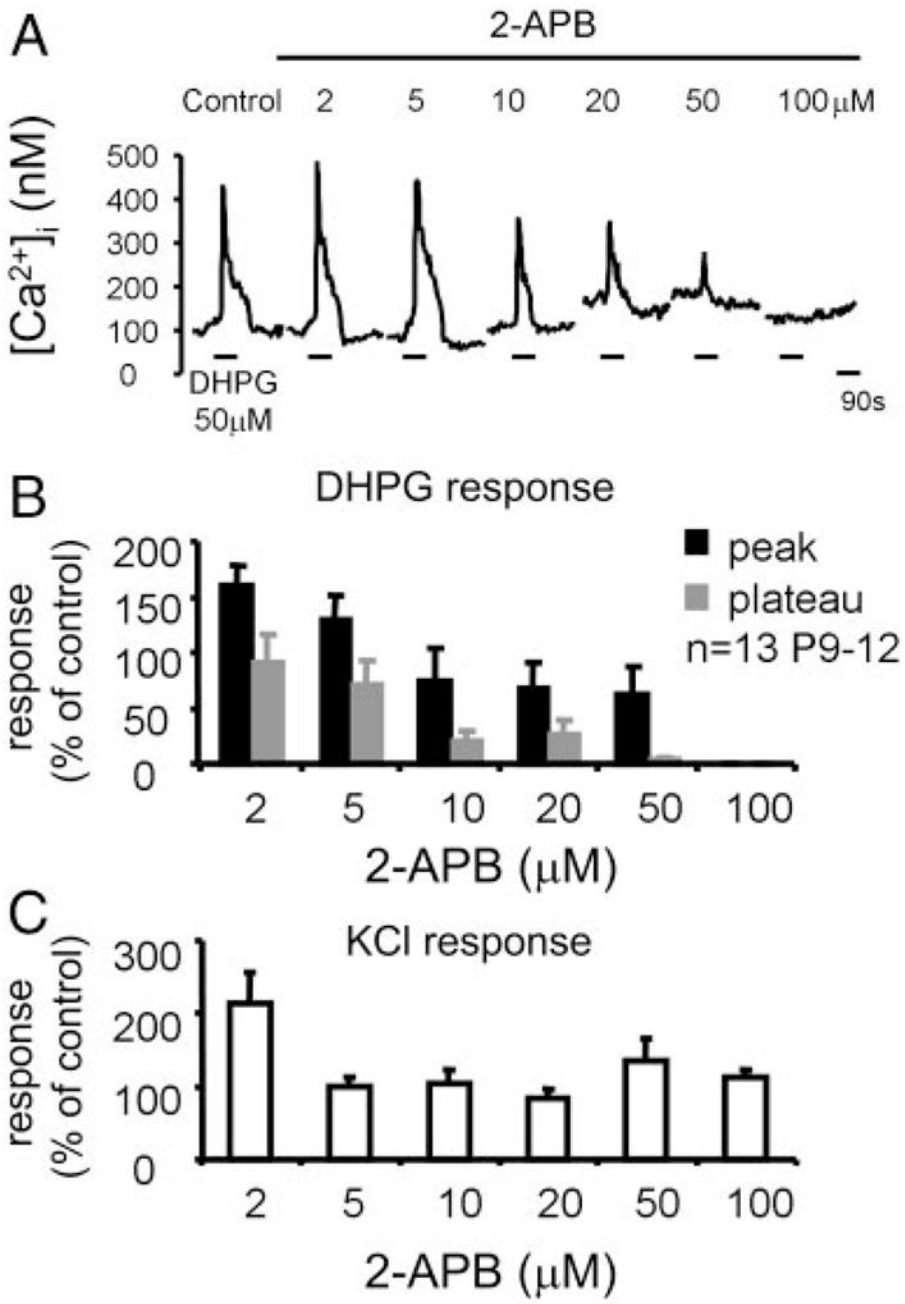

FIG. 5.

Effect of 2-aminoethoxydiphenylborane (2-APB) on group I mGluR-mediated Ca^{2+} responses. *A*: effect of increasing concentrations of 2-APB on DHPG-elicited Ca^{2+} responses in a P10 LSO neuron. *B*. summary data. *C*: effect of 2-APB on KCl-elicited (60 mM) Ca^{2+} responses. Data are from the same cells as in *B*.

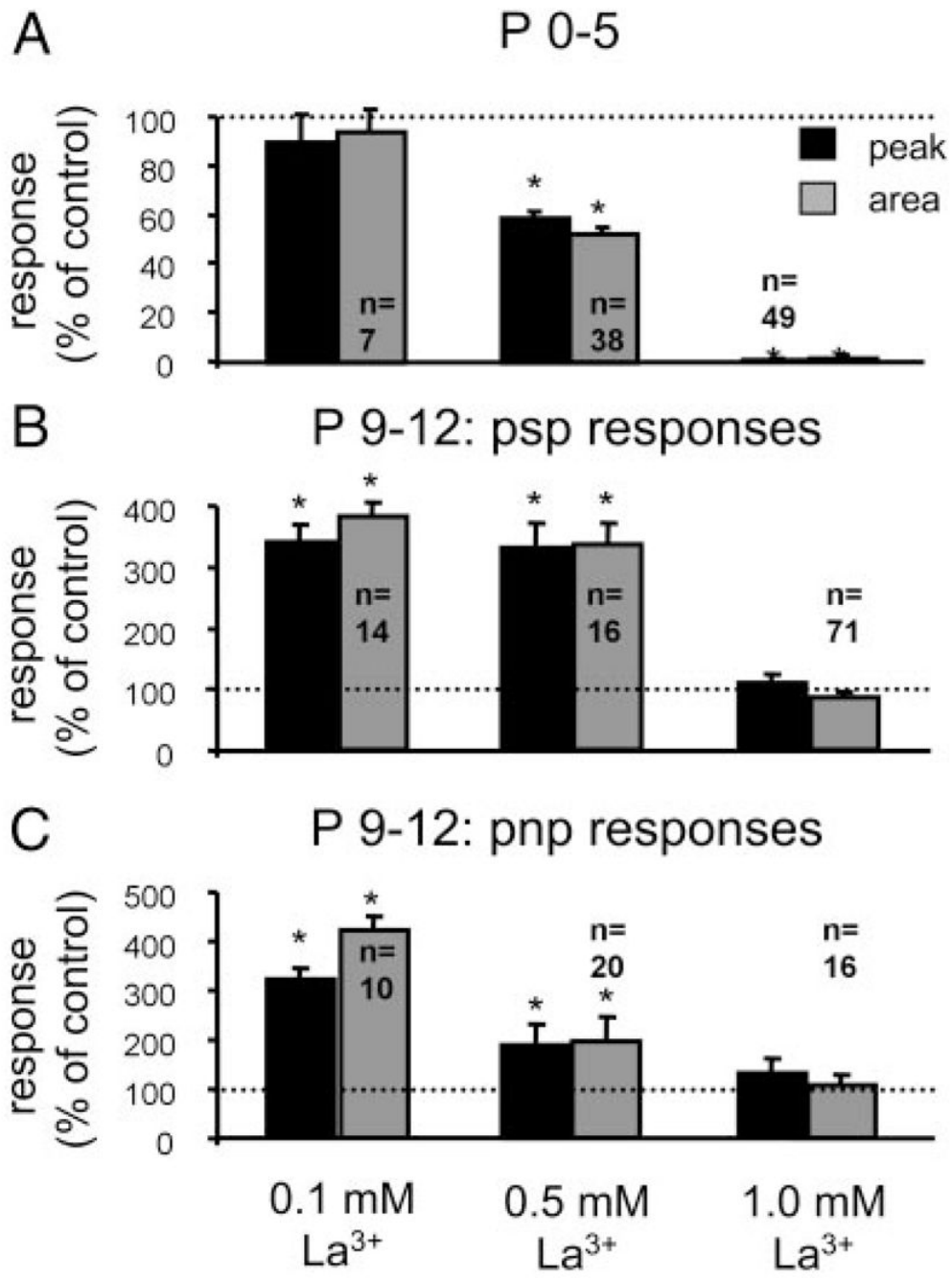

FIG. 6.

Effect of La^{3+} on group I mGluR-mediated Ca^{2+} responses. *A*: dose-dependent effect of La^{3+} on peak and area of DHPG-evoked (50 μM, 90 s) responses at P0–P5. *B* and C: in LSO neurons from P9–P12 mice (*B*: psp responses; *C*: pnp responses), La^{3+} potentiated responses at 0.1 and 0.5 mM, whereas it had no effect at 1.0 mM.

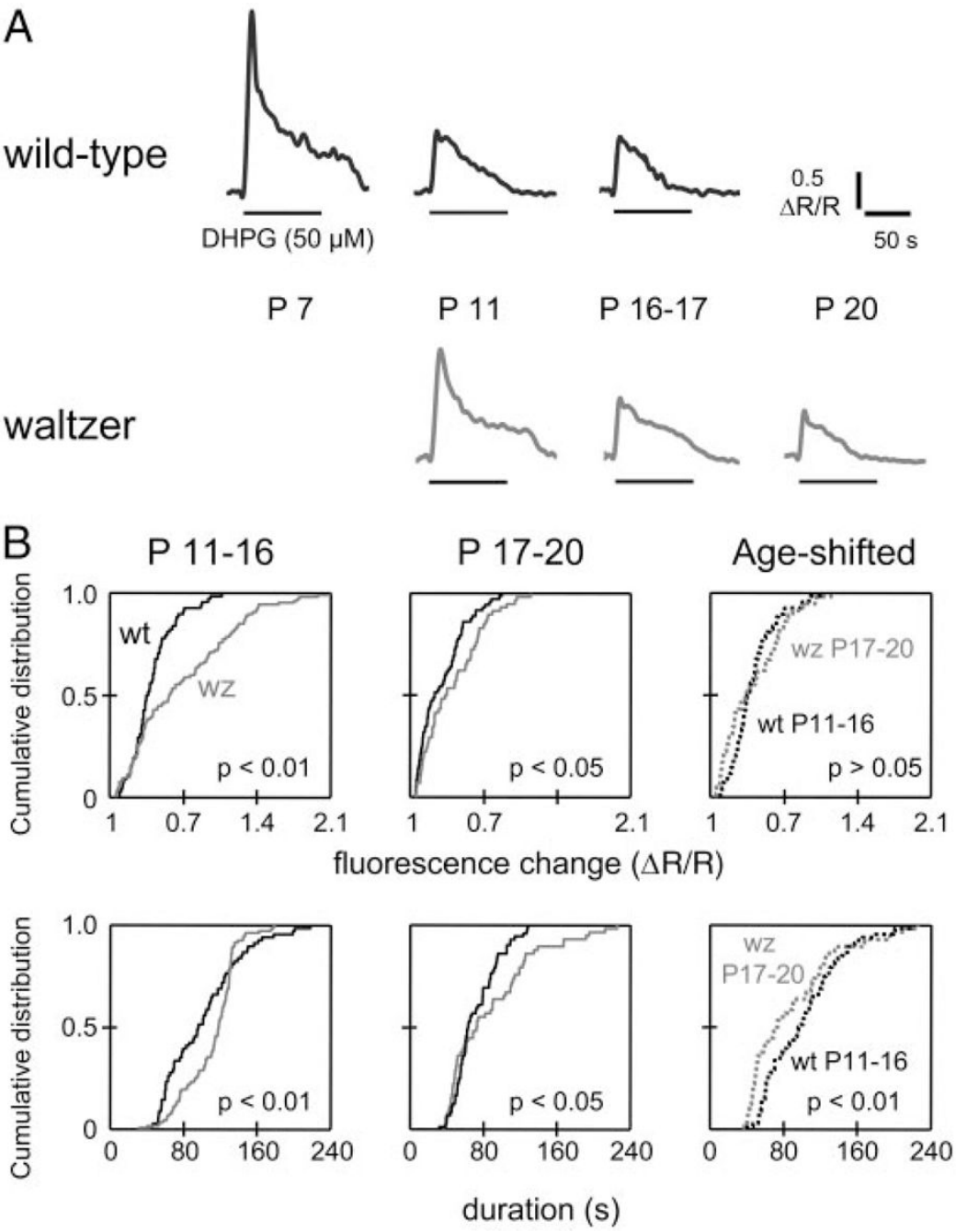

FIG. 7.

Group I mGluR-mediated Ca^{2+} responses in deaf waltzer mice. *A*: examples of DHPG-elicited Ca^{2+} responses in wild-type and waltzer mice. *B*: cumulative distribution plots of peak (*i*) and duration (*ii*) of DHPG-elicited responses of LSO neurons from wild-type (wt, black lines, P11–P16: $n = 68$ cells, P17–P20: $n = 72$ cells) and waltzer mice (wz, gray lines, P11–P16: $n = 107$ cells, P17–P20: $n = 58$ cells). *P* values for Kolmogorov–Smirnov (KS) test.

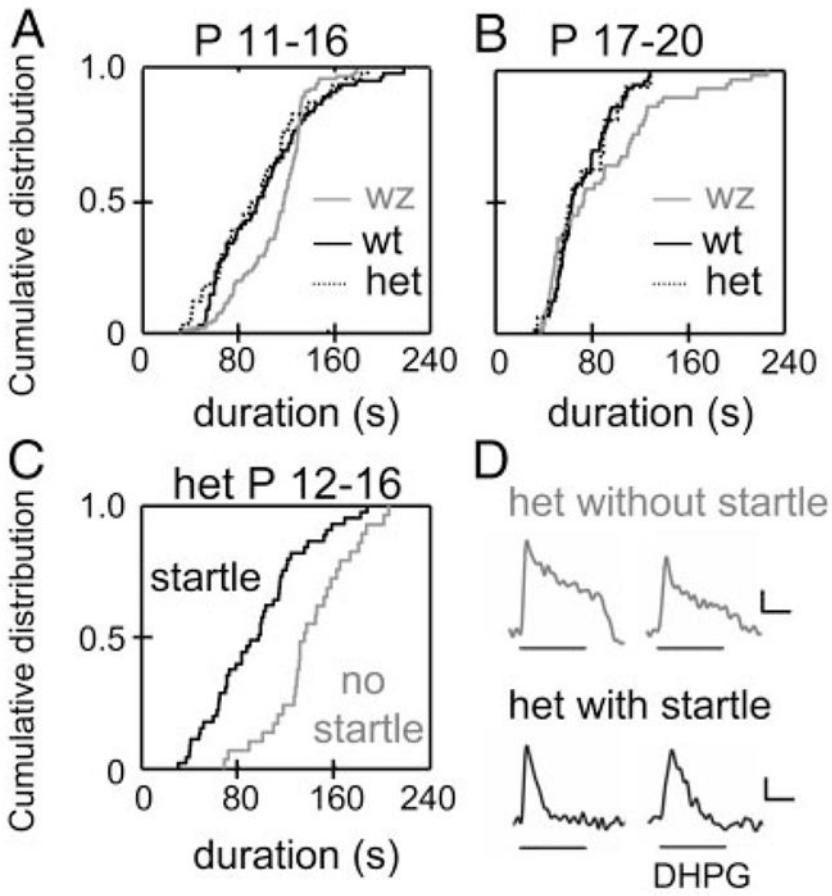

FIG. 8.

Durations of group I mGluR-mediated Ca^{2+}responses in waltzer, heterozygote, and wild-type mice. *A*: cumulative distribution of DHPG-elicited Ca^{2+} response durations in P11 to P16 LSO neurons from homozygote waltzer (wz, gray line, $n = 107$ cells), hearing heterozygote (het, dotted line, $n = 44$ cells), and hearing wild-type mice (wt, black line, $n = 68$ cells). Durations in heterozygote mice were significantly shorter compared with homozygote mice ($P < 0.005$) and were not different from wild-type mice ($P > 0.1$). *B*: same as *A* but for postnatal days 17–20. Durations in heterozygote mice were not significantly different from wild-type or homozygote mice (wz: $n = 58$ cells; het: $n = 16$ cells; wt: $n = 72$ cells). *C*: response durations in heterozygote mice with a startle response (black line; P14–P16, $n = 44$ cells) and mice lacking a startle response (gray line; P12–P13, $n = 29$ cells). Durations in mice lacking a startle response were significantly longer than in mice with a startle response ($P < 0.001$). *D*: examples of DHGP-elicited Ca^{2+}-responses from heterozygote mice with and without startle response. Scale bars, 0.02 ΔR/R (*top traces*), 0.01 ΔR/R (*bottom traces*), 50 s. *P* values for KS test.

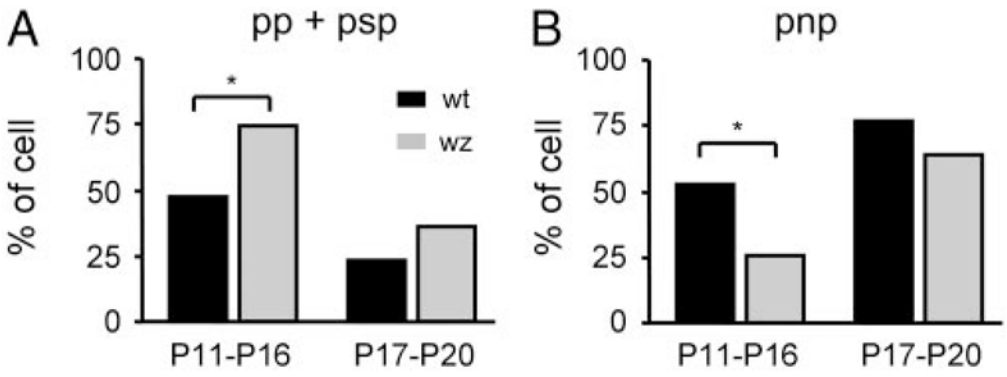

FIG. 9.

Developmental changes in response types in wild-type and waltzer mice. *A*: percentage of pp and psp responses is greater in wz than in wt mice for both age groups (P11–P16: wt = 32 cells, wz = 80 cells; Fisher's exact test, $P < 0.05$; P17–P20: wt = 17 cells, wz = 21 cells; Fisher's exact test, $P > 0.05$). *B*: percentage of pnp responses is smaller in wz than in wt mice (P11–P16: wt = 36 cells, wz = 27 cells; Fisher's exact test, $P < 0.05$; P17–P20: wt = 55 cells, wz = 37 cells; Fisher's exact test, $P > 0.05$)

TABLE 1

Parameters describing mGluR-elicited calcium responses in developing LSO neurons

	Peak and Plateau (pp) Group				Peak and Small Plateau (psp) Group			Peak and No Plateau (pnp) Group		
Age	P0–P5	P9–P12	P13–P16	P17–P19	P9–P12	P13–P16	P17–P19	P9–P12	P13–P16	P17–P19
N	222	178	132	54	178	132	54	178	132	54
n	222	46	15	4	75	42	7	59	75	43
n/*N*, %	100	24	11	7	42	32	12	32	57	80
Peak amplitude, nM	304 ± 15	247 ± 27	304 ± 51	90 ± 6	106 ± 13	138 ± 10	84 ± 1.5	56 ± 9	76 ± 6	51 ± 5
Plateau amplitude, nM	157 ± 7	97 ± 11	121 ± 20	51 ± 3	51 ± 4	46 ± 6	65 ± 13	—	—	—
Duration, s	190 ± 3	157 ± 5	167 ± 6	215 ± 8	129 ± 3	122 ± 4	172 ± 22	65 ± 3	76 ± 2	65 ± 3
Area, mM · s	25.9 ± 1.0	16.0 ± 1.8	26. ± 3 4.2	11.6 ± 0.3	8.3 ± 0.7	9.2 ± 0.7	11.9 ± 1.5	2.1 ± 0.3	3.1 ± 0.3	2.5 ± 0.4

Values are means ± SE. *N* = total number of cells tested; *n* = number of cells in a response group.